

Signatures for the second critical point in the phase diagram of a superconducting ring

Jorge Berger

Department of Physics, Technion, 32000 Haifa, Israel

Jacob Rubinstein

Department of Mathematics, Technion, 32000 Haifa, Israel

(Received 12 February 1997; revised manuscript received 2 April 1997)

We study the Little-Parks effect for families of mesoscopic loops with highly nonuniform thickness, using a recently developed formalism which predicts a phase diagram with two critical points at half-integer number of magnetic flux quanta. The Euler-Lagrange equation can be integrated analytically, and this feature provides an easy way to locate the second critical point and evaluate the derivative of the supercurrent. The derivative of the supercurrent (ac susceptibility) has been recently measured. Our results and experiments share the same qualitative features. [S0163-1829(97)00233-6]

We deal with a loop of superconducting material as in the Little-Parks experiment.^{1,2} We have recently predicted that, if the thickness of the loop is not exactly uniform, then there exist situations for which superconductivity is broken at a layer, so that the superconducting part is actually singly connected³ and no supercurrent flows. When this happens, we say that the sample is in the ‘‘singly connected state’’ (SC). This is an interesting possibility, since it would allow for a new dimensionality of the regions where the order parameter may vanish. In the case of vortices, the order parameter vanishes along lines and there are claims⁴ that it cannot vanish on surfaces. On the other hand, it has been suggested that even for uniform thickness the SC state will appear as an intermediate station in hysteretic paths.⁵ Some support for this possibility is provided by the energy barrier calculations used to fit the results in Ref. 6. A systematic analytic study for the stability domain of the SC state in families of loops with thicknesses that deviate slightly from uniformity was carried on in Ref. 7. Mathematical justification for some of the assumptions in our model was given in Ref. 8. A similar situation in which the order parameter seems to vanish on a layer was considered in Refs. 9 and 10.

The phase diagram in the temperature–magnetic-field plane⁷ is shown in Fig. 1. The axes are nondimensional quantities: $\lambda = (R/\xi)^2$, where R is the perimeter of the sample divided by 2π and ξ is the coherence length, and k is the deviation of the magnetic flux Φ from an integer, for Φ measured in units of $\Phi_0 = 2\pi\hbar c/e^*$. N (normal state), DC (doubly connected, in which the order parameter does not vanish), and SC denote the three possible states and Γ_I , Γ_{II} , and Γ_{III} are critical lines at which second-order phase transitions occur. The most prominent feature of this phase diagram is the existence of the point P_2 . When Γ_{III} is approached from below, the minimum of the order parameter decreases until it finally vanishes. Since Γ_{III} is located along $|k| = \frac{1}{2}$, and the most stable state is never at $|k| > \frac{1}{2}$, the SC stability domain is restricted to a line segment. The ends of this segment are the critical points P_1 and P_2 . When the magnetic field is varied and the line $|k| = \frac{1}{2}$ is crossed for small λ , the current I vanishes and changes sign continuously. However, beyond P_2 the current changes sign discontinuously. We

shall denote the positions of $P_{1,2}$ by $(\lambda = \lambda_{1,2}, |k| = \frac{1}{2})$; likewise, $T_{1,2}$ denote the respective temperatures. The parameter λ can be translated into temperature using²

$$\lambda = \frac{R^2}{\xi(0)^2} \frac{1 - (T/T_c)^2}{1 + (T/T_c)^2}, \tag{1}$$

where $\xi(0)$ is the coherence length at $T=0$ and T_c is the critical temperature in the absence of magnetic field.

A stationary state obeys the Euler-Lagrange equation. This is⁷

$$Dw w'' + D' w w' - \frac{D}{2} (w')^2 + 2\lambda D w^2 (1 - w) - \frac{2}{D} \left(\frac{2\pi k}{\Lambda} \right)^2 = 0, \tag{2}$$

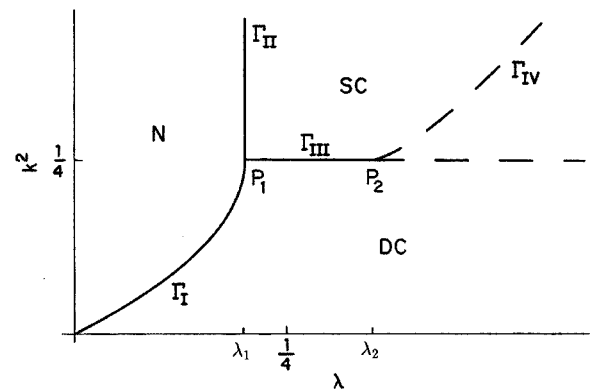


FIG. 1. Phase diagram. N: $w=0$; DC: $w>0$ everywhere; SC: the order parameter vanishes at some place in the loop and becomes singly connected. λ is a measure of the temperature below T_c and k^2 increases with the deviation from an integer number of flux quanta. Γ_I , Γ_{II} , and Γ_{III} are critical lines at which second-order transitions take place. P_1 and P_2 are critical points. For $\lambda > \lambda_2$ and $k^2 > \frac{1}{4}$ the DC state is still locally stable until Γ_{IV} is reached. Beyond Γ_{IV} there must be a decay to a situation with lower k^2 .

where w is the square of the normalized absolute value of the order parameter, derivatives are with respect to the angular coordinate θ , which is the arc length divided by R , and $D(\theta)$ is the cross section of the loop at θ ; Λ is defined by

$$\Lambda = \int_0^{2\pi} \frac{d\theta}{Dw}. \quad (3)$$

The analysis of Ref. 7 assumed that $D(\theta)$ is almost uniform and in this case the length $\lambda_2 - \lambda_1$ of the segment Γ_{III} turns out to be proportional to the deviation from uniformity (its first harmonic). On the other hand, for experimental purposes one would like the SC state to exist in a significant temperature range. We are therefore interested in the case that $D(\theta)$ is strongly nonuniform. In general, this situation requires numerical integration of Eq. (2), but analytic integration is possible in the case that $D(\theta)$ is piecewise constant, as considered in the following.

A piecewise constant thickness will be described by $D(\theta)$ of the form

$$D = \begin{cases} D_1 \equiv d & \theta < \theta^*, \\ D_2 \equiv 1 & \theta^* < \theta < \pi, \end{cases} \quad (4)$$

with $0 < d = D_1/D_2 < 1$ and $0 < \theta^* < \pi$ constants, and $D(\theta)$ symmetric about $\theta = 0$ and about $\theta = \pi$. [When evaluating the order parameter we are free to set $D_2 = 1$, since the Euler-Lagrange equation is invariant under multiplication of $D(\theta)$ by a constant.]

A model similar to Eq. (4) was used long ago¹¹ to evaluate the current through a Josephson junction in the framework of the Ginzburg-Landau theory. Besides mathematical simplicity, the piecewise constant thickness case turns out to give the largest length $\lambda_2 - \lambda_1$ among the families of thickness profiles which we have studied.¹² At first sight, it could be suspected that the one-dimensional formalism on which Eq. (2) and the phase diagram in Fig. 1 rely might not apply to the piecewise constant case. The reason is that mathematical proofs for the justification of the one-dimensional formalism assume⁸ that $D(\theta)$ is smooth; intuitively, it can be said that near the region where the thickness changes the streamlines are strongly curved and the current density cannot be nearly constant in the entire cross section. However, further study shows that the phase diagram in Fig. 1 can still be obtained by means of a two-dimensional analysis¹³ and that the results obtained for the piecewise constant thickness appear to be the limit of those obtained for families of smooth functions.

In the piecewise constant case we have found a solution of Eq. (2) with the appropriate symmetry, with a minimum at $\theta = 0$ and a maximum at $\theta = \pi$. It has the form

$$w(\theta) = \begin{cases} A_1 - \frac{2\nu_1^2}{\lambda} m_1 \text{cn}^2(\nu_1 \theta, m_1), & \theta < \theta^*, \\ A_2 - \frac{2\nu_2^2}{\lambda} m_2 (1 - m_2) \text{sd}^2(\nu_2(\pi - \theta), m_2), & \theta > \theta^*. \end{cases} \quad (5)$$

Here cn and sd are Jacobian elliptic functions,¹⁴ ν_i and m_i are constants, and

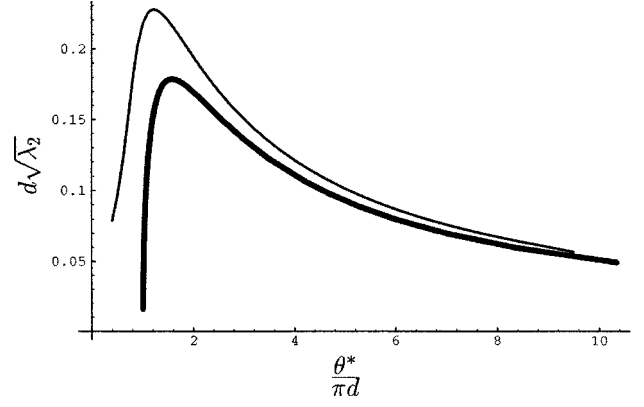


FIG. 2. Position of P_2 for the shape (4). Thick line: asymptotic result for $d \leq 1$. Thin line: $d = 0.1$.

$$A_i = \frac{2}{3} \left(1 + (2m_i - 1) \frac{\nu_i^2}{\lambda} \right). \quad (6)$$

The constant term in Eq. (2) becomes

$$\left(\frac{2\pi k}{D_i \Lambda} \right)^2 = \frac{A_i}{8\lambda} [\lambda^2 (A_i - 2)^2 - 4\nu_i^4]. \quad (7)$$

Equations (5)–(7) reduce the integrodifferential equation (2) to the problem of determining the four constants ν_i and m_i . We are thus left with four algebraic equations: Eq. (7) for $i = 1, 2$ and continuity of w and Dw' at $\theta = \theta^*$. These equations are solved by Newton iterations and the integration in Eq. (3) is performed numerically.

In this way we obtain the curves in Fig. 2, which describe λ_2 as a function of the length of the thin piece for given d . These curves suggest that large domains of stability for the SC state may be found, provided that the dimensions of the thin piece are properly tuned. A simple interpolation formula for the length of the thin piece that maximizes λ_2 is

$$\frac{\theta^*(d)}{\pi} = \frac{0.734d}{0.468 + d}. \quad (8)$$

We claim now that signatures of the singly connected state have already been observed by means of ac susceptibility measurements.^{15,6} This is surprising, since the phase diagram in Fig. 1 is expected only for rings with nonuniform thickness. These susceptibility measurements were intended to be done on rings with uniform thickness, but some (unknown) nonuniformity must have been present.

According to our predictions, above T_2 the supercurrent vanishes when Φ/Φ_0 is either integer or half-integer. Therefore, we expect the area under the curve in a plot of $dI/d\Phi$ against Φ to vanish for each half-period above this temperature, but not below T_2 . Indeed, Fig. 4 of Ref. 15 is in complete qualitative agreement with this prediction and with the phase diagram in Fig. 1. Near T_c there is no hysteresis; hysteresis appears only below some temperature which may be identified as T_2 .

For the purpose of qualitative comparison with Fig. 4 in Ref. 15 we arbitrarily consider now a piecewise constant loop with $d = \theta^*/\pi = \frac{1}{4}$. We do not attempt a quantitative treatment, since some of the relevant quantities have still not

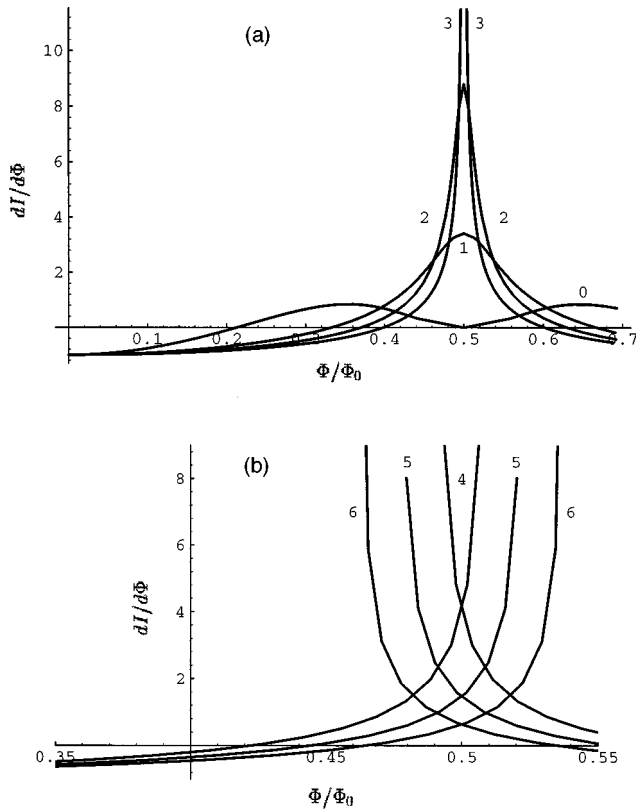


FIG. 3. Derivative of the induced supercurrent with respect to the enclosed magnetic flux. The curves are shown as functions of the flux, with λ as a parameter. These curves were calculated for a piecewise constant cross section, with $d = \theta^*/\pi = \frac{1}{4}$. For this example, the critical points $P_{1,2}$ are located at $\lambda_1 = 0.105$ and $\lambda_2 = 1.35$. The values of λ were taken as $\lambda = \lambda_1 + n(\lambda_2 - \lambda_1)/3$, where the integer n is shown next to each curve. The curves were normalized through division by the value of $|dI/d\Phi|$ at $\Phi = 0$, which is $(c\lambda D_2)/(14\pi^2\kappa^2 R^3)$. (a) $\lambda \leq \lambda_2$. As λ approaches λ_2 , the peak at $\Phi = \Phi_0/2$ becomes higher and narrower. At $\lambda = \lambda_2$, it diverges. (b) $\lambda > \lambda_2$. Here hysteresis is possible. As λ increases beyond λ_2 , the cusp at $\Phi = \Phi_0/2$ becomes less pronounced.

been measured and, besides, the experiment used a very wide ring that requires a two-dimensional analysis.

As discussed by Zhang and Price,¹⁵ the response to ideal ac susceptibility measurements is proportional to the derivative of the supercurrent with respect to the magnetic flux. The supercurrent is⁷

$$I = \frac{c\Phi_0\lambda}{4\pi\kappa^2 R^3} \frac{k}{\Lambda}, \quad (9)$$

where κ is the ratio between the penetration depth λ_L and the coherence length ξ , and the fraction k/Λ appears in Eq. (7). The derivative of I can now be obtained by differentiating Eqs. (9), (3), and (5)–(7).

The result is shown in Fig. 3. The resemblance with the experimental results is encouraging. Agreement is found not only in the presence or absence of hysteresis, but also in the trend of the temperature dependence of the height and width of the peaks, both above and below T_2 .

A complementary case which can be studied is that of a ring with nearly uniform cross section. We obtain that the

ratio between the values of $dI/d\Phi$ at $\Phi = \Phi_0/2$ and at $\Phi = 0$ is $4(\lambda - \lambda_1)/(\lambda - \lambda_2)$ for $\lambda_1 \leq \lambda < \lambda_2$ and $2(\lambda_1 - \lambda_2)/(\lambda - \lambda_2)$ for $\lambda > \lambda_2$ and $\lambda \approx \lambda_2$. In spite of the very different chosen shape, this is again in qualitative agreement with the piecewise constant case and with the experimental results.

The identification of $dI/d\Phi$ in Fig. 3 with the measured ac susceptibility corresponds to the ideal limit of small ac amplitude and high frequency. In a real experiment, three kinds of deviations are expected. First, I is not a linear function of Φ in the range probed by the ac field; this difficulty is most serious when $dI/d\Phi$ has a narrow peak or a discontinuity, which will be smeared. In Ref. 15 the amplitude is about $0.05\Phi_0$; this imperfection should be added to the fact that the ring is very wide, so that different paths along it enclose considerably different fluxes.

Second, if the probed region corresponds to a metastable state and if the ac cycle is not fast compared to the lifetime, then decays and hysteresis will occur and the experimental results will deviate from the adiabatic ac susceptibility described by Fig. 3. As the ac frequency is lowered, the results approach isothermal susceptibility. And third, no matter how high the frequency is, decays and hysteresis must occur if the ac amplitude extends the probed region in Fig. 1 beyond Γ_{IV} .

If the temperature is lower than but very close to T_2 , then the energy barrier and the distance between $|k| = \frac{1}{2}$ and Γ_{IV} are very small. Therefore, decays will occur in this region. These decays produce a discontinuity in I , which is experimentally similar to the divergence of $dI/d\Phi$. It follows that the results in this region may appear similar to those immediately above T_2 . In order to approach the theoretical situation, measurements ought to be repeated at various ac amplitudes and frequencies and then extrapolated to the ideal limit.

Measurements of the ac susceptibility in mesoscopic rings have also been performed by Davidović *et al.*⁶ These measurements were performed at much lower frequencies than in Ref. 15, but this has no qualitative influence on the results considered here. In this case the system was a large array of rings with magnetic interaction, but the authors conclude that the paramagnetic peaks at $\Phi_0/2$ are a single-ring effect. Again, the height of this peak goes through a maximum at some temperature T_p , which we may identify as T_2 averaged over the rings. Moreover, it is found that T_p corresponds roughly to a “freezing temperature.” This is precisely what is expected from our interpretation: below T_2 there is an energy barrier for changing the direction of the supercurrent, whereas above T_2 there is no barrier. Further agreement with our interpretation is provided by their Fig. 8: the susceptibility depends on the frequency below T_2 , but not above T_2 . Our explanation is that at low frequencies rings have time to decay to the state with reversed current, but above T_2 there is nowhere to decay.

As discussed in the previous paragraphs, hysteresis in the probing cycle is present only in a limited region, immediately below T_2 . Since an experimental signature for hysteresis is an imaginary component in the ac susceptibility, T_2 could be characterized by the onset of this component as the temperature is lowered. The maximum value of this imagi-

nary component and the temperature at which it is located depend on the amplitude and frequency of the ac field.

The intermediate state used in Ref. 6 to calculate the energy barrier, which is needed for their fit, is the continuation of our SC state, taken to the limit of a uniform ring and corrected for nonzero self inductance. For $\lambda > \lambda_2$ this state is a saddle point and for $\lambda < \lambda_2$ it is stable. However, for a strictly uniform ring, λ_1 and λ_2 coalesce and the SC state is never stable.

The experiments in Refs. 15 and 6 were not planned for verifying the range of existence of the singly connected su-

perconducting state. As a consequence, the available data are insufficient for a quantitative fit and we cannot rule out other possible explanations for the paramagnetic peak. However, for a purposely designed experiment,¹² ac susceptibility offers a sensitive tool for revealing the critical point at $\Phi = \Phi_0/2$ and $T = T_2$.

We wish to thank John Price for sending us the experimental data of Ref. 15 and Daniel Reich for sending us the unpublished results of Ref. 6. This research was supported by the U.S.-Israel Binational Science Foundation. J.B. was also supported by the Israel Science Foundation.

-
- ¹W. A. Little and R.D. Parks, Phys. Rev. Lett. **9**, 9 (1962); R. D. Parks and W. A. Little, Phys. Rev. **133**, A97 (1964); R. P. Groff and R. D. Parks, *ibid.* **176**, 567 (1968).
- ²M. Tinkham, *Introduction to Superconductivity* (McGraw-Hill, New York, 1996).
- ³J. Berger and J. Rubinstein, Phys. Rev. Lett. **75**, 320 (1995).
- ⁴C. M. Elliott, H. Matano, and T. Qi, Eur. J. Appl. Math. **5**, 431 (1994).
- ⁵E. M. Horane, J. I. Castro, G. C. Buscaglia, and A. López, Phys. Rev. B **53**, 9296 (1996).
- ⁶D. Davidović *et al.*, Phys. Rev. B **55**, 6518 (1997).
- ⁷J. Berger and J. Rubinstein, SIAM J. Appl. Math. (to be published).
- ⁸J. Rubinstein and M. Schatzman, J. Math. Pure Appl. (to be published).
- ⁹H. J. Fink, A. López, and R. Maynard, Phys. Rev. B **26**, 5237 (1982); H. J. Fink, V. Grünfeld, and A. López, *ibid.* **35**, 35 (1987); H. J. Fink, J. Loo, and S. M. Roberts, *ibid.* **37**, 5050 (1988).
- ¹⁰V. V. Moshchalkov, L. Gielen, M. Dhallé, C. Van Haesendonck, and Y. Bruynserade, Nature (London) **361**, 617 (1993).
- ¹¹A. Baratoff, J. A. Blackburn, and B. B. Schwartz, Phys. Rev. Lett. **25**, 1096 (1970).
- ¹²J. Berger and J. Rubinstein, Physica C (to be published).
- ¹³J. Berger and J. Rubinstein (unpublished).
- ¹⁴*Handbook of Mathematical Functions*, edited by M. Abramowitz and I. A. Stegun, U.S. Natl. Bureau of Standards (U.S. GPO, Washington, DC, 1964).
- ¹⁵X. Zhang and J. C. Price, Phys. Rev. B **55**, 3128 (1997).